Dynamical phase transitions in periodically driven model neurons

Jan R. Engelbrecht[1] and Renato Mirollo[2]

[1]*Department of Physics, Boston College, Chestnut Hill, Massachusetts 02467, USA*
[2]*Department of Mathematics, Boston College, Chestnut Hill, Massachusetts 02467, USA*

Transitions between dynamical states in integrate-and-fire neuron models with periodic stimuli result from tangent or discontinuous bifurcations of a return map. We study their characteristic scaling laws and show that discontinuous bifurcations exhibit a kind of phase transition intermediate between continuous and first order. In the model-independent spirit of our analysis we show that a six-dimensional (6D) gating variable model with an attracting limit cycle has similar phase transitions, governed by a 1D return map. This reduction to 1D map dynamics should extend to real neurons in a periodic current clamp setting.

Neurons in awake, behaving mammals receive complicated dendritic input currents and respond with highly irregular trains of action potentials. Unraveling the meaning of each neuron's train of spikes is a formidable challenge. There is a long history of detecting collective rhythmic neural activity at various scales, from electroencephalography (EEG), to local field potentials, to oscillatory membrane currents stimulating individual pyramidal and interneurons in voltage clamp recordings. Yet the general question of how collective rhythmic activity in a network affects an individual neuron's spike timing is far from well understood. We present a biophysical approach to this problem that is informed by the theory of phase transitions in statistical mechanics, emphasizing universal features in the spike-timing patterns and in their development. Real neurons are very complicated but such universal features that are independent of the approximation inherent in modeling provide the link between theory and experiment.

Consider a neuron in a slice preparation firing at some rate, and then subsequently injected with an additional small rhythmic stimulus current. The neuron will then adjust its spike times, and in some instances may speed up or slow down enough to entrain to the rhythm. More generally one can study the dependence of a neuron's firing pattern on a periodic input current. Extensive theoretical work [1–5] on this problem, typically using integrate-and-fire models, developed the notion of p-q entrainment, where the neuron fires exactly q times over p cycles of the rhythm, which can be described in terms of the dynamics of a (possibly discontinuous) return map that relates successive neuron spike times. Complementary studies incorporating coupled pairs or networks of neurons [6,7], transmission delays [8], noise [9], and threshold modulation [10] have contributed to a substantial literature on this topic. A related set of recordings on squid giant axons receiving only periodic pulses with an analysis using the FitzHugh-Nagumo model demonstrated [11] the practicality of a return-map analysis in real cells.

In this paper we cast this analysis in the framework of phase transitions and demonstrate that the entrainment plateaux have various universal, model-independent features. We show that the convergence to entrainment to a p-q phase-locked firing pattern is characterized by one of two sets of very particular scaling relations. These two universality classes originate from the two possible bifurcations of the return map associated with entrainment. One of these bifurcations leads to a new kind of phase transition, intermediate between the continuous and first-order transitions traditionally encountered in statistical mechanics. Most significantly, it turns out that this analysis applies not only to one-dimensional (1D) threshold models but also to multidimensional neuron models based on dynamical gating variables, since a 1D return map essentially governs the dynamics despite a much higher-dimensional state space. The order associated with entrainment originates in the return map becoming periodic in the presence of rhythmic stimuli. This principle also applies to real neurons and consequently an analysis of electrophysiological data in terms of a return map would explore to what extent the universal features across different models also manifest in living cells.

We begin by considering a generic 1D threshold model of a neuron's response to the influx of a current $I(t)$. The cell's membrane voltage $v(t)$ is governed by a differential equation of the form $Cdv/dt=f(v)+I(t)$, together with the condition that if $v(t)$ reaches a threshold v_{th} then an instantaneous action potential or "spike" is generated and $v(t)$ is reset to an equilibrium resting potential v_{eq}. The constant C is the membrane capacitance. We take as the initial condition some time t_0 and $v(t_0)=v_{\text{eq}}$. The neuron's response is then characterized by its train of spike times $t_0,t_1,t_2,\ldots$; the relationship between consecutive spike times determines a return map F via $t_n=F(t_{n-1})=F^n(t_0)$. In the simplest case where $I(t)$ is constant, the neuron fires periodically and the interspike interval (ISI) $t_n-t_{n-1}=T_0$ is constant, provided $I(t)=I_0$ is above the threshold I_{th} which insures $\dot{v}>0$ for $v_{\text{eq}}\leq v(t)\leq v_{\text{th}}$. In other words, the return map is simply $F(t)=t+T_0$.

Next we add a periodic perturbation to the constant current case: for example, $I(t)=I_0+I_1\cos(2\pi t/T_{\text{dr}})$. The return map F is no longer a simple linear function, but satisfies the periodicity relation $F(t+T_{\text{dr}})=F(t)+T_{\text{dr}}$ reflecting the periodicity of the perturbation. We impose the condition $I_1<f(v_{\text{eq}})+I_0$, which guarantees that $v(t)$ never drops below v_{eq}. Under this condition, either all solutions $v(t)$ with initial condition $v(t_0)=v_{\text{eq}}$ eventually reach the threshold v_{th}, or none do [again due to the periodicity of $I(t)$]. In the spiking case F is strictly increasing, and continuous when $I_1<f(v_{\text{th}})+I_0$. Typically $f(v_{\text{th}})<f(v_{\text{eq}})$ so we expect to find discontinuous maps for sufficiently small I_0, as noted in Ref. [3].
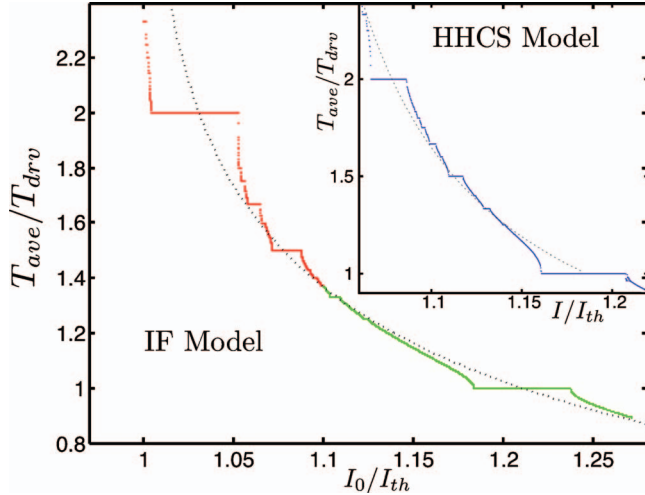
FIG. 1. (Color) Ratio of average period to rhythm period for the IF model vs I_0 for amplitude $I_1=0.1I_{th}$, $\tau=20$ ms, and $T_{dr}=35$ ms. The dotted curve is the ISI in the undriven case and the inset is for the HH-CS model with $I_1=0.14I_{th}$.

The introduction of a second, competing time scale leads to a loss of the simple periodic behavior of the original model. The model neuron typically no longer has a constant interspike interval, and can exhibit both periodic and aperiodic firing patterns. The asymptotic dynamics are determined by the average ISI

$$T_{av} = \lim_{n\to\infty} \frac{t_n}{n} = \lim_{n\to\infty} \frac{F^n(t_0)}{n}. \tag{1}$$

We know from circle map theory [1,2,12] that the limit defining T_{av} exists, is independent of t_0, and depends continuously on all parameters. Furthermore, the dimensionless ratio T_{av}/T_{dr} is a rational number $r=p/q$ if and only if

$$F^q(t^*) = t^* + pT_{dr} \tag{2}$$

for some t^*; in other words t^* is a fixed point of the map $F^q(t)-pT_{dr}$. So the spike train beginning with $t_0=t^*$ satisfies $t_{n+q}=t_n+pT_{dr}$ and consequently the sequence of phases of t_n relative to T_{dr} repeats every q firings.

A simple example of this is the classic leaky integrate-and-fire (IF) model which has $f(v)=-(v-v_{eq})/R$. The membrane resistance R together with C determine a time constant $\tau=RC$. This particular model has $I_{th}=(v_{th}-v_{eq})/R$. In Fig. 1 we plot T_{av}/T_{dr} for the IF model as a function of the parameter I_0, while keeping fixed $T_{dr}=35$ ms, $\tau=20$ ms, and I_1

$=0.1I_{th}$. We divide the graph into two regions according to whether the return map is continuous (green) or discontinuous (red).

The asymptotic structure of the average firing rate as in Fig. 1 has been known for some time [1–3]. In this paper our focus is on the approach to the asymptotic behavior, the resulting connection to dynamical phase transitions and subsequent universal characteristics. For a given number r, let M_r^- and M_r^+ denote the minimum and maximum values of I_0 for which $T_{av}/T_{dr}=r$. Then $M_r^- < M_r^+$ if and only if r is a rational number; in other words the plateaux in Fig. 1 correspond to rational multiples of the drive period. We view Fig. 1 as a phase diagram, with each plateau a state corresponding to some rational number $r=p/q$.

Within each p/q entrainment plateau, the spike train converges to a pattern of ISIs that repeats every q spikes, corresponding to a stable fixed point t^* of $F^q(t)-pT_{dr}$. For perfect p/q entrainment $t_{n+q}-t_n-pT_{dr}=0$; hence

$$\Delta_n^{p,q} = t_{n+q} - t_n - pT_{dr} \tag{3}$$

measures the deviation from p/q entrainment. The convergence (in a plateau) is geometric: $\Delta_n^{p,q} \sim [(F^q)'(t^*)]^n$.

The fixed points of $F^q(t)-pT_{dr}$ vary with I_0 and ultimately vanish through some kind of bifurcation at the edges of the p/q entrainment plateau. Analogous to the theory of phase transitions, the equation

$$\Delta_n^{p,q} \sim e^{-n/\xi_\tau(I_0)} \tag{4}$$

defines a coherence time $\xi_\tau(I_0)$ that characterizes how rapidly the phase-locked solution is approached. Of particular interest is how $\xi_\tau(I_0)$ scales with respect to the tuning parameter I_0 as an edge of an entrainment plateau (phase boundary) is approached. As we shall show, the scaling has a universal form dictated by the type of bifurcation through which the fixed points are lost.

We first analyze the phase transitions and scaling behaviors in the parameter range where F is continuous, as in Fig. 2(a). Upon varying I_0 the fixed point is here lost through a tangent bifurcation. The generic behavior near such a phase boundary can be modeled by the simple map $g(x)=x-x^2+\lambda$, which has a stable fixed point at $x^*=\sqrt{\lambda}$ that is lost through a tangent bifurcation as $\lambda\to0^+$. Let $\delta x_n=x_n-x^*$; then $\delta x_{n+1}-\delta x_n=-2\sqrt{\lambda}\,\delta x_n-(\delta x_n)^2$, which has large n solution $\delta x_n \sim \exp(-2\sqrt{\lambda}n)$ so $x_n\to x^*$ with a coherence time $\xi \sim 1/\sqrt{\lambda}$. This generic scaling holds for each fixed point of $F^q(t)-pT_{dr}$ and as the phase boundary is approached from within a plateau the coherence time then scales as
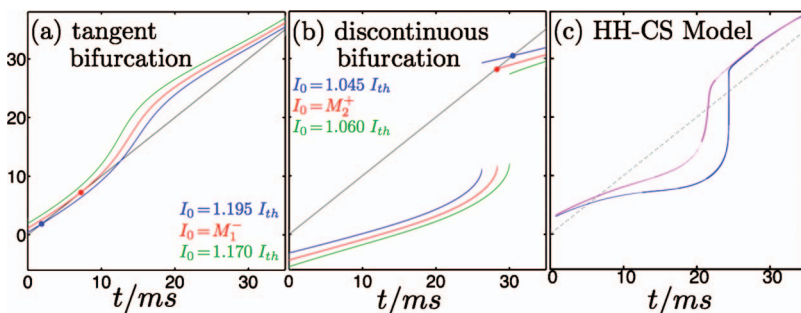
FIG. 2. (Color) Return maps $F(t)-pT_{dr}$ for the IF model for $I_1/I_{th}=0.1$ near (a) left edge of $r=1$ plateau and (b) right edge of $r=2$ plateau. Return map for (c) the HH-CS model for $I_1/I_{th}=0.07$ and for 0.14 with I_0 inside the $r=2$ plateau.
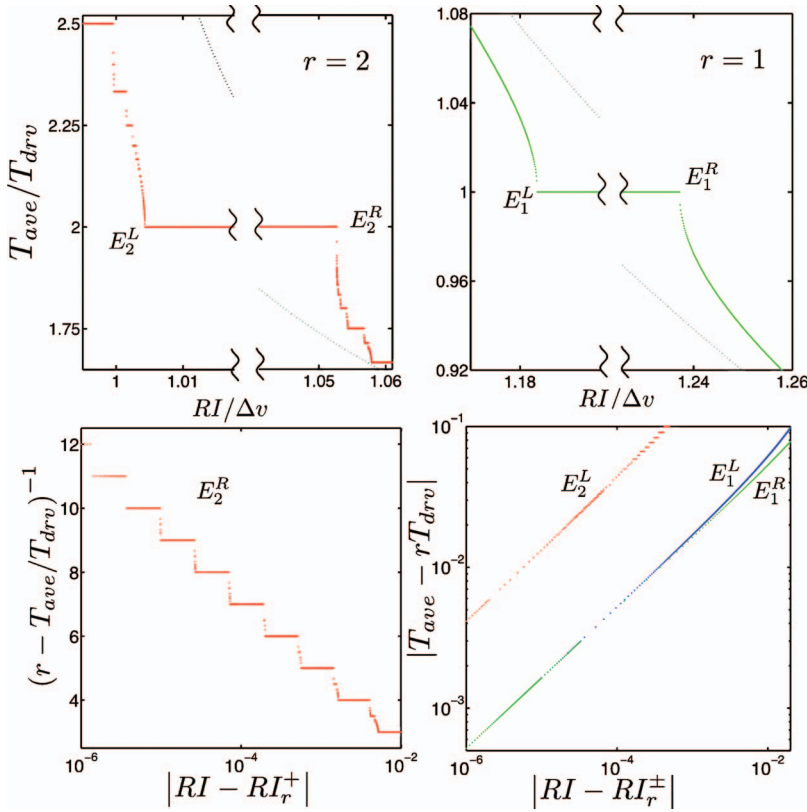
FIG. 3. (Color) Scaling in T_{av} near the edges of the $r=2$ and $r=1$ plateaux. Edge E_2^R demonstrates the logarithmic scaling in Eq. (8) at a discontinuous bifurcation, while edges E_2^L, E_1^L, and E_1^R exhibit power law scaling in Eq. (7) at tangent bifurcations.

$$\xi_\tau(I_0) \sim \frac{1}{|I_0 - M_r^\pm|^{1/2}} \qquad (5)$$

consistent with classical exponent $\nu = \frac{1}{2}$ in equilibrium critical phenomena [15].

The coherence time diverges at the phase boundary (when the control parameter $I_0 = M_r^\pm$), and the dynamics can again be modeled by the map $g(x)$. In this case $\lambda = 0$, the fixed point $x^* = 0$ and the δx_n^2 term above becomes relevant. The large n solution is now $x_n \sim 1/n$ and hence $x_{n+1} - x_n \sim -1/n^2$; in particular the fixed point at the tangent bifurcation is no longer approached geometrically. Analogously, the p/q-entrainment coherence at the phase boundary then develops according to the power law

$$\Delta_n^{p,q} \sim \frac{1}{n^2} \qquad (6)$$

consistent with a critical exponent $\eta = 0$.

As we vary the control parameter I_0 so as to exit the p/q entrainment plateau, convergence to a fixed point is replaced by arbitrarily slowly evolving dynamics near the locations of the q lost fixed points which we casually refer to as "bottlenecks." The dynamics can again be modeled by the map $g(x)$ which has a bottleneck near $x = 0$ for small negative λ. As $\lambda \to 0^-$, the number of iterations N_λ needed to pass through a fixed interval $[-c, c]$ around zero scales such as $N_\lambda \sim 1/\sqrt{|\lambda|}$. N_λ characterizes how long in takes to pass through a single bottleneck and introduces a time scale outside the entrainment plateau that diverges similar to the coherence time in Eq. (5). The deviation of the average period from rT_{dr} is inversely proportional to the number of iterations required

to pass through the bottleneck due to a lost fixed point of $F^q(t) - pT_{dr}$; thus

$$|T_{av} - rT_{dr}| \sim |I_0 - M_r^\pm|^{1/2}. \qquad (7)$$

This average deviation of entrainment plays the role of a disorder parameter which, in analogy to phase transitions, identifies the exponent $\beta = \frac{1}{2}$. This scaling form is illustrated in Fig. 3.

In the parameter range where F is discontinuous it can also acquire or lose periodic points through a discontinuous bifurcation. As we shall see, the associated scaling near the phase boundaries for these bifurcations belongs to a new universality class. An example of this type of bifurcation is illustrated in Fig. 2(b), for $r = 2$. The behavior at the bifurcation (phase boundary) depicted here differs fundamentally from the continuous case in Fig. 2(a), in that the slope of the map at the fixed point here remains strictly less than 1. Iterates of the map still converge to the fixed point following the geometric form in Eq. (4), corresponding to a finite coherence time at the bifurcation, as opposed to power law scaling.

The behavior near the plateau edges for discontinuous bifurcations can be modeled by the piecewise-linear discontinuous map $h(x) = ax + \lambda$ for $x > 0$ and $h(x) = x - 1$ for $x < 0$, where $0 < a < 1$ is fixed and λ varies through 0. Let $\tilde{x} = \lambda/(1-a)$; $\tilde{x}$ is the unique fixed point of h for $\lambda \geq 0$. This fixed point is lost as $\lambda \to 0^+$ in a bifurcation similar to that seen in Fig. 2(b). Since h is linear for $x > 0$, successive iterates satisfy $x_n = h^n(x_0) = \tilde{x} + a^n(x_0 - \tilde{x})$ provided $x_0, \ldots, x_{n-1} > 0$. A bottleneck near $x = 0$ develops for λ small negative, and even though $\tilde{x} < 0$ is then no longer a fixed point of h, it

still controls the passage through the bottleneck in terms of the expression for x_n above. The number of iterations N_λ needed to pass through an interval $[0, c]$ is determined by solving $0 = \tilde{x} + a^s(c - \tilde{x})$ for s and rounding up to the nearest integer ($N_\lambda = \lceil s \rceil$). Substituting $\tilde{x} = \lambda/(1-a)$ gives $a^s = -\lambda/[(1-a)c - \lambda]$. Therefore, as $\lambda \to 0^-$, $s \sim \ln(-\lambda)/\ln a$ so N_λ scales as $-\ln|\lambda|$.

By analogy, for I_0 just outside the edge of a plateau at which a discontinuous bifurcation occurs, the number of iterations required to pass through the bottleneck due to the lost fixed point of $F^q(t) - pT_{dr}$ scales as $-\ln|I_0 - M_r^\pm|$. As before, the deviation of the average period from rT_{dr} is inversely proportional to this and thus scales as

$$|T_{av} - rT_{dr}| \sim \frac{-1}{\ln|I_0 - M_r^\pm|}. \tag{8}$$

So our disorder parameter vanishes logarithmically at phase boundaries determined by discontinuous bifurcations—slower than any power law.

For the IF example, both types of bifurcations do occur in the parameter range where F is discontinuous. In fact, a more careful analysis (based on monotonicity and concavity properties of F) proves that discontinuous bifurcations occur only at the right edges of the entrainment plateaus, so all left-edge bifurcations are tangent. Right-edge bifurcations come in both types although tangent bifurcations are quite rare. For example, in Fig. 1 tangent bifurcations occur at the right edges of the plateaux for $r = \frac{3}{2}$, $\frac{7}{5}$, and $\frac{11}{8}$; all other right-edge bifurcations we investigated in this parameter range are discontinuous. Moreover, it can be shown that the bifurcations at the right edges are all discontinuous for I_0 below some threshold, if the oscillatory drive I_1 is small relative to I_{th}.

The dynamical transitions discussed above are analogous to equilibrium phase transitions in statistical physics. For example, the scaling laws at tangent bifurcations are equivalent to the laws for continuous phase transitions with classical exponents $\beta = \frac{1}{2}$, $\nu = \frac{1}{2}$, and $\eta = 0$, where singular (and universal) behavior results from a diverging coherence scale. The behavior at discontinuous bifurcations is unusual, mixing properties of both continuous and first order transitions: while the disorder parameter $T_{av} - rT_{dr}$ vanishes continuously at the bifurcation, the coherence time remains finite. The singularity underlying universality is the discontinuity in the map, leading to a logarithmic scaling law for $T_{av} - rT_{dr}$ that vanishes more slowly than any power law.

Now we demonstrate how the preceding analysis can apply to multidimensional nonlinear gating variable neuron models. Consider the canonical Hodgkin-Huxley equations with stimulus current $I(t) = I_0 + I_1 \cos(2\pi t/T_{dr})$ and an additional Connor-Stevens A-current term [13]

$$C\frac{dv}{dt} = -g_{Na}m^3h(v - E_{Na}) - g_K n^4(v - E_K) - g_L(v - E_L)$$

$$-g_A a^3 b(v - E_A) + I_0 + I_1 \cos(2\pi t/T_{dr}). \tag{9}$$

The ODEs describing the gating variables $n(t)$, $m(t)$, $h(t)$, $a(t)$, and $b(t)$ and the values of the constants C, g_{Na}, g_K, g_A, g_L, E_{Na}, E_K, E_A, and E_L are taken from Ref. [14]. In the unperturbed case ($I_1 = 0$) the A-current term causes arbitrarily long ISIs for I_0 above a stimulus threshold I_{th}, as in the IF model [here we define the spikes as $v(t)$ increasing through zero]. The HH-CS model exhibits an entrainment pattern strikingly similar to the IF model, as shown in the inset of Fig. 1 where we plot the average ISI vs I_0 in units of I_{th} for this model. We again use $T_{dr} = 35$ ms but now take a slightly larger $I_1 = 0.14I_{th}$. For larger I_0 one can see square root scaling near the plateau edges, and for smaller I_0 the plateaux become more stairlike, reminiscent of the discontinuous bifurcations discussed above.

At first glance, our 1D map analysis should not apply since the voltage and five gating variables evolve in a 7D state space (including time). But if we plot consecutive spike times (t_n, t_{n+1}) for a large number of different initial conditions we do essentially recover a one-dimensional map as shown in Fig. 2(c). This can be explained as follows. It is known that the unperturbed system ($I_1 = 0$) has an attracting limit cycle for $I_0 > I_{th}$, which becomes an attracting cylinder in the 7D state space that includes time. This attracting invariant surface persists, at least for small $I_1 > 0$. Spikes occur when trajectories cross the 1D curve $v = 0$ on this surface, so the map is just the Poincaré return map for this section.

For $I_1 = 0$ the return map is $F(t) = t + T_0$, where T_0 is the period of the system's limit cycle. As we increase I_1 above zero, the shape of F changes continuously but quite rapidly as illustrated in Fig. 2(c). For example, even for relatively modest I_1, the maximum slope of F can be large ($>10^5$ for $I_1 = 0.14I_{th}$ and I_0 in the $r = 2$ plateau). When this happens, the resulting T_{av} curve resembles the discontinuous case studied in the IF model. Thus, even though F may still technically be continuous, our analysis of the phase transitions at discontinuous bifurcations is relevant and moreover helps explain the dominance of the plateaux in the blue curve in the inset in Fig. 1.

In conclusion, periodically driven 1D threshold neurons lose p-q entrainment through two markedly different routes, corresponding to tangent and discontinuous bifurcations. Each has its own characteristic universal scaling laws which measure the rate of convergence to entrainment within the p-q plateau as well as the deviation from p-q entrainment just outside the plateau. Remarkably, this 1D map analysis also applies to higher-dimensional gating variable models. From a neurophysiological perspective, our results suggest that when a neuron firing at some rate receives an additional rhythmic perturbation, spike timing adjusts according to a return map. Whole-cell slice recording is an ideal setting in which to explore *in vitro* the pattern formation discussed in this paper.

[1] B. W. Knight, J. Gen. Physiol. **59**, 734 (1972).

[2] J. P. Keener, Trans. Am. Math. Soc. **261**, 589 (1980).

[3] J. P. Keener, F. C. Hoppenstead, and J. Rinzel, SIAM J. Appl. Math. **41**, 503 (1981).

[4] S. Coombes and P. C. Bressloff, Phys. Rev. E **60**, 2086 (1999); S. Coombes, M. R. Owen, and G. D. Smith, *ibid.* **64**, 041914 (2001); C. Laing and S. Coombes, Int. J. Bifurcation Chaos Appl. Sci. Eng. **15**, 1433 (2004).

[5] K. Pakdaman, Phys. Rev. E **63**, 041907 (2001).

[6] P. C. Bressloff and S. Coombes, Phys. Rev. Lett. **80**, 4815 (1998); **81**, 2168 (1998); **81**, 2384 (1998); SIAM J. Appl. Math. **60**, 820 (2000); P. C. Bressloff, S. Coombes, and B. de Souza, Phys. Rev. Lett. **79**, 2791 (1997).

[7] J. Rubin and A. Bose, Physica D **221**, 37 (2006); Network Comput. Neural Syst. **15**, 133 (2004).

[8] P. C. Bressloff and S. Coombes, Physica D **126**, 99 (1999); **130**, 232 (1999).

[9] P. H. E. Tiesinga, J. V. José, and T. J. Sejnowski, Phys. Rev. E **62**, 8413 (2000); P. H. E. Tiesinga, *ibid.* **65**, 041913 (2002); P. H. E. Tiesinga, J. M. Fellous, and T. J. Sejnowski, Neurocomputing **44**, 195 (2002).

[10] T. Gedeon and M. Holzer, J. Math. Biol. **49**, 577 (2004).

[11] D. T. Kaplan, J. R. Clay, T. Manning, L. Glass, M. R. Guevara, and A. Shrier, Phys. Rev. Lett. **76**, 4074 (1996).

[12] R. L. Devaney, *An Introduction to Chaotic Dynamical Systems* (Addison Wesley, New York, 1989).

[13] J. A. Connor and C. F. Stevens, J. Physiol. (London) **213**, 21 (1971).

[14] P. Dayan and L. F. Abbott, *Theoretical Neuroscience* (MIT, Cambridge, MA, 2001).

[15] N. Goldenfeld, *Lectures on Phase Transitions and the Renormalization Group* (Addison-Wesley, New York, 1992).